IEICE TRANS. ELECTRON., VOL.E88–C, NO.5 MAY 2005

INVITED PAPER *Joint Special Section on Recent Progress in Optoelectronics and Communications*

Erbium-Doped Lithium Niobate Waveguide Lasers

Wolfgang SOHLER[†a)], **Bijoy K. DAS**[†], **Dibyendu DEY**[†], **Selim REZA**[†], **Hubertus SUCHE**[†], *and* **Raimund RICKEN**[†], *Nonmembers*

SUMMARY The recent progress in the field of Ti:Er:$LiNbO_3$ waveguide lasers with emission wavelengths in the range 1530 nm $< \lambda <$ 1603 nm is reviewed. After a short discussion of the relevant fabrication methods concepts and properties of different types of lasers with grating resonator, acoustooptically tunable Fabry Pérot type lasers and new ring laser structures are presented.

key words: *integrated optics, lithium niobate, rare earth, erbium, waveguide lasers*

1. Introduction

During the last years there was a considerable interest in rare-earth doped $LiNbO_3$ waveguide lasers. In particular, a whole family of Er-doped waveguide lasers of excellent quality has been developed emitting in the wavelength range 1530 nm $< \lambda <$ 1603 nm. Free running lasers of the Fabry Pérot type, harmonically mode-locked lasers (5 ps/10 GHz), Q-switched lasers (4 ns/1 kHz/1 kW), Distributed Bragg Reflector- (DBR-) lasers, self-frequency doubling devices, and acoustooptically tunable lasers have been reported [1], [2].

Er:$LiNbO_3$ is an excellent laser material for integrated optics. It can be easily fabricated in the surface layer of a $LiNbO_3$ substrate by indiffusion of a thin vacuum-deposited Er layer. Afterwards, a single mode channel waveguide is defined by the standard indiffusion technique of Ti-stripes. If optically pumped by $\lambda = 1480$ nm radiation a wavelenth dependent gain of up to 2 dB/cm results.

Additional doping by Fe allows to define holographically waveguide gratings of excellent quality. Reflectivities $> 95\%$ and a spectral halfwidth of the grating characteristic of < 60 pm enabled the development of narrow linewidth integrated optical DBR- [3], Distributed Feedback- (DFB-) [4], and coupled DBR-DFB-lasers [5].

Acoustooptically tunable lasers have been significantly improved during the last years. As example, a 47 nm tuning range has been demonstrated [6]. Moreover, a tunable frequency shifted feedback laser with a variety of remarkable properties has been developed [7].

The first ring laser in Er:$LiNbO_3$ was demonstrated a few months ago using a Ti-indiffused waveguide structure [8]. Such a ring laser has a great potential to be used as compact laser gyro.

It is the aim of this contribution to review the recent progress in the field of Ti:Er:$LiNbO_3$ waveguide lasers. In particular, we will present different types of integrated lasers with grating resonators, acoustooptically tunable Fabry Pérot type lasers and new ring laser structures.

2. Laser Fabrication

The fabrication of Erbium-doped waveguide lasers in $LiNbO_3$ consists of a sequence of steps, starting with diffusion doping of the substrate, followed by waveguide and resonator fabrication. Electrooptically and acoustooptically intracavity controlled devices require corresponding electrode structures and waveguides for surface acoustical waves (SAWs), respectively. Small bandwidth resonators for DBR- and DFB-lasers can be developed with etched surface relief or photorefractive gratings; the latter require an additional doping e.g. by Fe. In this section the different fabrication steps are briefly described.

Erbium-doping: The electronic transitions of Er^{3+}:$LiNbO_3$ exploited for lasing around 1550 nm wavelength represent a quasi three level system with ground state absorption. Therefore, Er-doping should be restricted to pumped sections of an integrated optical device; otherwise, strong absorption sets in. Such a selective doping cannot be achieved during crystal growth; it can only be achieved by indiffusion of a patterned, vacuum-deposited Er-layer [9]. This technique proved to be ideally suited for waveguide laser development avoiding clustering of Er-ions in the $LiNbO_3$ host. Moreover, it is compatible with Ti-indiffusion for waveguide fabrication.

Er-diffusion doping of $LiNbO_3$ follows Fick's laws resulting in a nearly Gaussian concentration profile [9]. It allows to obtain concentration levels up to the solid solubility limit (about 0.18 at% at 1060°C, the waveguide fabrication temperature) without fluorescence quenching [10]; this is a prerequisite for significant optical gain in a short device (up to 2 dB/cm has been demonstrated experimentally). Due to the low diffusivity of the Er^{3+}-ions, high diffusion temperatures up to 1130°C (close to the Curie temperature of ferroelectric $LiNbO_3$) and long diffusion times (up to 150 h, depending on crystal orientation) are required. For acoustooptically tunable lasers and for DFB- and DBR-lasers Er is diffused into X-cut wafers, whereas for electrooptically

Manuscript received January 10, 2005.

[†]The authors are with the Department of Physics, Faculty of Science, University of Paderborn, 33095, Paderborn, Germany.

a) E-mail: sohler@physik.uni-paderborn.de

DOI: 10.1093/ietele/e88–c.5.990

modelocked and Q-switched lasers it is diffused into Z-cut wafers. Due to the low ion mobility Er-diffusion doping is always the first step of doped waveguide fabrication.

Acoustical waveguide fabrication: If an acoustooptically controlled waveguide laser is to be developed intracavity acoustooptical filter and frequency shifter have to be fabricated in the next step. As Ti-doping changes the elastical properties of the $LiNbO_3$ substrate it can be used to design waveguides for surface acoustic waves (SAWs). Ti-doped "claddings" of very high concentration are indiffused (e.g. 160 nm/1060°C/24 hrs) to form an undoped SAW-guiding channel of 100 μm width [11]. Interdigital electrode structures of about 17 μm periodicity, photolithographically defined in vacuum-deposited Al-layers, allow an efficient excitation of SAWs at a frequency of about 170 MHz; they can propagate with losses as low as 0.3 dB/cm. The width of 100 μm of a SAW-waveguide allows to incorporate along its axis an optical waveguide, which is considerably narrower. In this way a combined acoustical/optical waveguide can be formed yielding a nearly ideal overlap of acoustical and optical fields. This results in an optimum efficiency of all acoustooptical interactions.

Optical waveguide fabrication: Several technologies such as proton exchange, Ti-indiffusion or Zn-diffusion can be used for waveguide fabrication in $LiNbO_3$. However, in proton exchanged, Er-doped waveguides a dramatic fluorescence quenching (radiative lifetime reduction) has been observed due to the coupling to OH-phonons [12].

Up to now high quality Er-doped waveguides have only been fabricated by Ti-indiffusion. The resulting channel guides provide single-mode guiding in both, TE- and TM-polarization, which is mandatory e.g. for the acoustooptically tunable laser. The fluorescence lifetime of the upper laser level of 2.7 ms is almost identical to the one of bulk Er:$LiNbO_3$.

Single-mode waveguides for wavelengths around 1550 nm are fabricated by indiffusion (9 h/1060°C) of 7 μm wide, 100 nm thick Ti-stripes, photolithographically defined on the surface of the $LiNbO_3$ substrate. For Q-switched and modelocked lasers the waveguides are fabricated on Z-cut substrates with propagation along the X-axis to utilize the largest electrooptic coefficient for intracavity modulation and to take advantage of the higher optical gain in this crystal orientation. For acoustooptically tunable lasers and for DBR-/DFB-lasers X-cut substrates are used to allow efficient surface acoustic wave (SAW) excitation and grating fabrication, respectively. For the former ones propagation is along the Y-axis, whereas for the latter ones propagation is along Z (polar axis).

Fe-doping: If photorefractive gratings are required to form the cavity of DBR- or DFB-lasers, an additional Fe-doping is necessary to increase the photorefractive sensitivity of $LiNbO_3$ [13] in selected sections of a Ti-doped optical waveguide with or without additional Er-doping. In these sections a refractive index grating of sub-μm periodicity can be

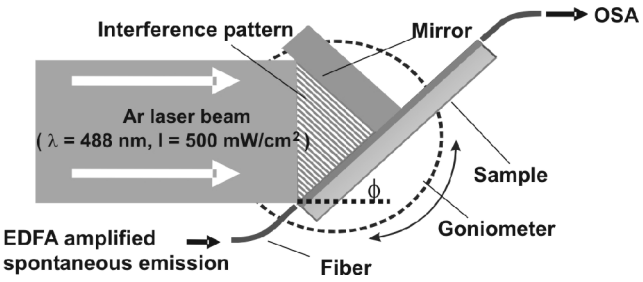

Fig. 1 Holographic setup to write a photorefractive grating in a Ti:Fe:(Er:)$LiNbO_3$ channel guide with online monitoring of the generated Bragg-response around λ = 1550 nm.

easily fabricated holographically. Fe^{2+} acts as a donor for photoionized carriers whereas Fe^{3+} acts as a trap. Charge separation is mainly driven by the photovoltaic effect, which is strongest along the Z-axis [14]. Therefore, optical waveguides for DFB- and DBR-lasers are delineated along Z.

Typically, about 15 mm long sections of a waveguide are sensitized by indiffusion (70 h/1060°C) of a vacuum-deposited Fe-layer of about 40 nm thickness leading to a concentration profile of about 40 μm 1/e depth [15]. After indiffusion the sample is annealed in a wet Ar-atmosphere to provide the necessary proton concentration for the fabrication of fixed holographic gratings.

Holographic grating definition: Photorefractive gratings are written using a holographic (two beam interference) setup (see Fig. 1). A "Lloyd" arrangement provides a wavefront splitting and intersection of the expanded collimated beam of an Ar-laser (λ=488 nm) on the waveguide surface generating a periodic light pattern [16]. Optically excited electrons move into the dark regions of the periodic light pattern, where they are trapped, generating a periodic space charge field. This periodic field induces a refractive index grating via the electrooptic effect; the resulting Bragg response is measured during holographic illumination by monitoring with an optical spectrum analyzer (OSA) the transmitted amplified spontaneous emission of an Erbium Doped Fiber Amplifier (EDFA) through the waveguide.

However, due to a residual dark conductivity of $LiNbO_3$ the electronic space charge pattern decays with time after the holographic illumination is switched off. This serious problem can be overcome by "fixing" the grating [17] taking advantage of the mobility of protons at elevated temperatures (~180°C). The mobile protons compensate the electronic space charge and generate a positive replica. After cooling to room temperature the ionic space charge distribution with the resulting field is "frozen," but the electronic one can be "smoothed" using a constant homogeneous illumination with blue light. In this way stable Bragg gratings can be fabricated; peak reflectivities of the Bragg response of up to 60% and a bandwidth of 60 pm have been achieved [15].

Dielectric mirror deposition: Dielectric mirrors are needed for resonator definition of tunable, modelocked and Q-

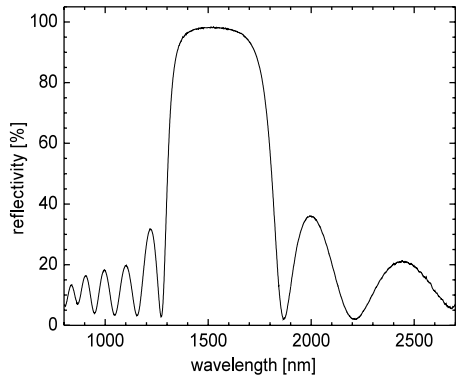

Fig. 2 Measured reflectivity versus wavelength of a dielectric mirror comprised of 12 layers of quarterwave thickness at 1550 nm wavelength.

switched lasers with a Fabry Perot type cavity. They are comprised of alternating SiO_2 and TiO_2 quarterwave layers directly deposited onto the polished waveguide endfaces. O_2-ion beam assisted e-beam evaporation is used to fabricate fully oxidized (non absorbing) layers of high density at low substrate temperatures. Figure 2 shows a typical reflectivity spectrum of a dielectric mirror comprised of 12 layers.

3. DBR- and DFB-Lasers

Several types of narrow linewidth lasers with optical feedback by photorefractive gratings have been developed: distributed Bragg reflector- (DBR-) [3], distributed feedback- (DFB-) [4], and DBR-/DFB-coupled cavity lasers [5] with single mode Ti:Er:$LiNbO_3$ waveguide. They have one or two photorefractive gratings in Fe-doped waveguide sections.

Two types of DBR-lasers have been demonstrated. One has a cavity consisting of one Bragg-grating, a gain section, and a multi-layer dielectric mirror deposited on the opposite waveguide end face. The other DBR-cavity consists of two gratings in Ti:Fe:$LiNbO_3$ waveguide sections on both sides of the Er-doped waveguide (see Fig. 3(a)) [3]. Single-frequency operation could be achieved in the latter case at various wavelengths in the Er-band (1530 nm < λ < 1575 nm) with up to 1.12 mW output power (see Figs. 3(b) and 3(c)).

The DFB-laser has a thermally fixed photorefractive grating in a Ti:Fe:Er:$LiNbO_3$ waveguide section; it is combined with an integrated optical amplifier on the same substrate. Up to 1.12 mW of output power at λ = 1531.35 nm was emitted by the laser/amplifier combination at a pump power level of 240 mW (λ_P = 1480 nm). The emission spectrum consists of the two lowest-order DFB-modes of about 3.9 GHz frequency spacing [4].

Moreover, an attractive DBR/DFB coupled cavity laser has been developed (see Fig. 4) [5]. The laser consists of a photorefractive Bragg grating in the Ti:Fe:Er:$LiNbO_3$ waveguide section (a DFB-laser) close to one end face of the sample, a Ti:Er:$LiNbO_3$ gain section and a broadband multi-layer dielectric mirror of high reflectivity on

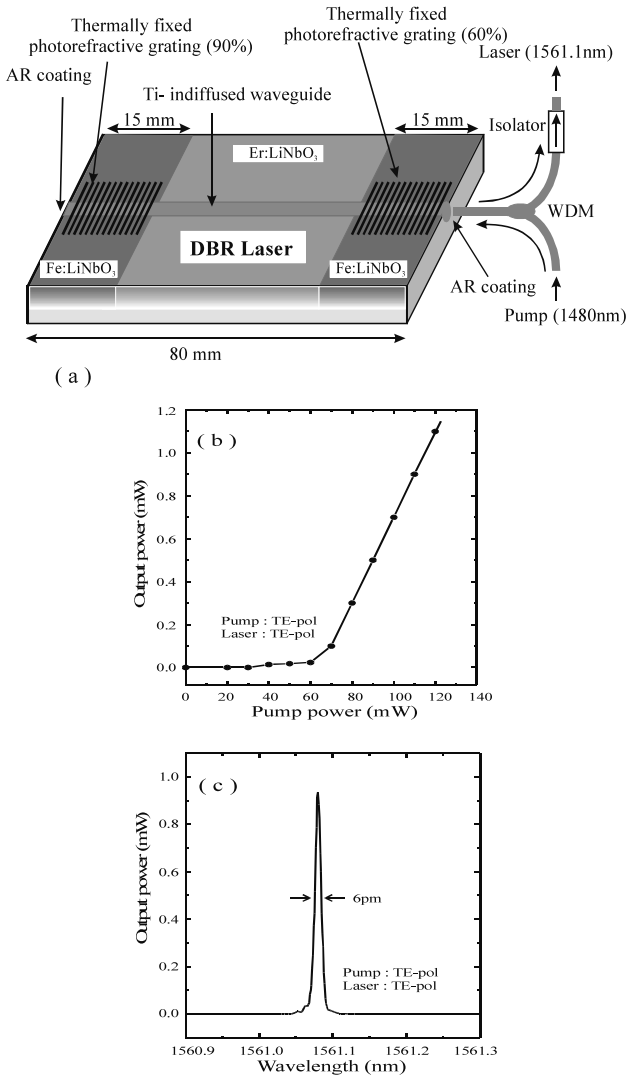

Fig. 3 (a) Schematic structure of a DBR-laser with a cavity comprised of two thermally fixed photorefractive gratings. (b) Power characteristics. (c) Emission spectrum.

the other end face. Single-frequency operation has been achieved with an output power of up to 8 mW. The optically pumped (λ_p = 1480 nm, P = 130 mW) laser emits up to 8 mW at λ = 1557.2 nm with a slope efficiency of about 22%. The single-frequency laser emission wavelength can be thermo-optically and electro-optically tuned by a fraction of a nanometer.

4. Acoustooptically Tunable Lasers

4.1 Narrow Linewidth Laser

A diode-pumped packaged acousto-optically tunable integrated Ti:Er:$LiNbO_3$ waveguide laser was reported by Schäfer et al. [18] in 1997. It could be tuned (not continuously) over 31 nm in the wavelength range 1530 nm < λ < 1610 nm with an emission linewidth of 0.3 nm. Recently, an improved version has been developed with a modified

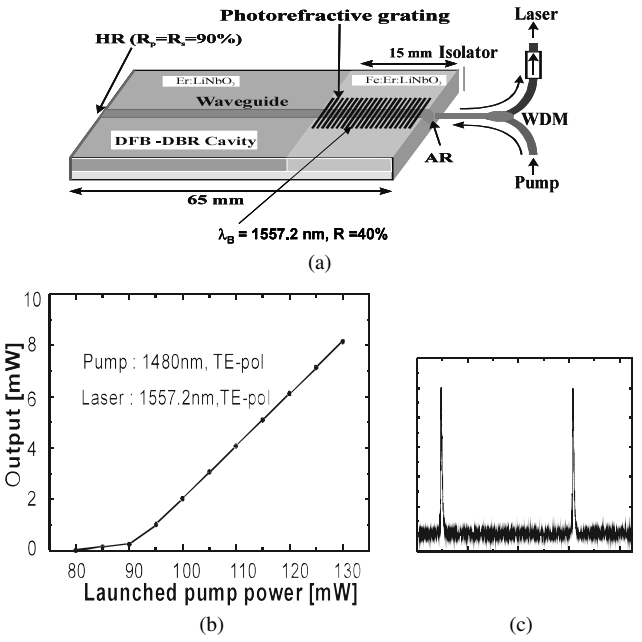

Fig. 4 (a) Schematic structure of a coupled cavity DBR-/DFB-laser. (b) Power characteristics. (c) High resolution emission spectrum (Fabry-Pérot measurement).

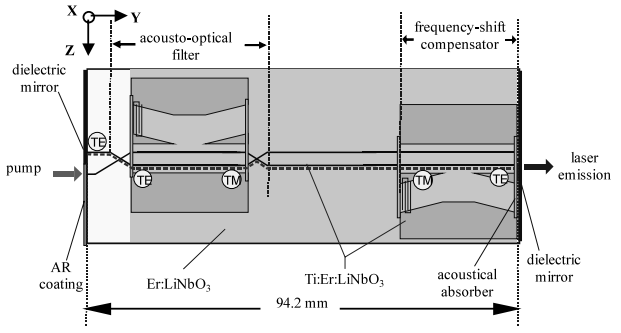

Fig. 5 Schematic diagram of the acoustooptically tunable waveguide laser.

design (see Fig. 5) [6]. The laser consists of an integrated acoustooptical filter incorporated in the Er-doped amplifyer section, an acoustooptical frequency-shift compensator and dielectric end face mirrors defining the waveguide resonator. The acoustooptical filter is composed of two polarization splitters and an acoustooptical polarization converter with a tapered acoustooptical directional coupler in between. A certain wavelength is selected by an acoustooptical polarization conversion. As this process is determined by phase matching it is strongly wavelength selective with a (interaction length dependent) filter bandwidth of about 1 nm. Due to the interaction with a running SAW a frequency shift of about 170 MHz is imposed on the optical wave by passing the acoustooptical filter. This frequency shift has to be compensated during each round trip in a conventional laser. Therefore, an additional acoustooptical polarization converter, which serves as frequency shift compensator, is incorporated in the waveguide cavity. The resonant optical field inside the laser resonator undergoes four times a polarization conversion during each round trip and follows the dotted line in Fig. 5 through the waveguide polarization splitters. A TM polarized pump is necessary to ensure pumping of the Er-doped waveguide along this path leading to TE polarized laser output. On the other hand, a TE polarized pump will excite the path along the upper waveguide inside the filter and leads to a TM polarized laser output; all the polarization states will be orthogonal to those given in Fig. 5. For TM polarized pump (λ_p = 1480 nm), the laser threshold is 45 mW at 1561 nm output wavelength; a maximum output power of 0.5 mW is observed at 135 mW pump power.

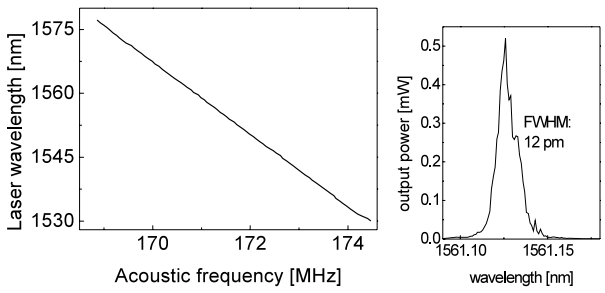

Fig. 6 (Left) Tuning characteristic of the acoustooptically tunable laser as emission wavelength versus SAW frequency of acoustooptical filter and frequency shift compensator. (right) Emission spectrum.

The laser tuning range could be extended to 47 nm (see Fig. 6). The output wavelength is changed by adjusting the acoustic frequency of the intracavity acoustooptical filter and frequency-shift compensator; the tuning slope is about 8.2 nm/MHz. If appropriate operating conditions are adjusted a linewidth smaller than 12 pm can be observed, measured with an optical spectrum analyzer of 10 pm resolution bandwidth. Therefore, a much smaller true linewidth can be assumed corresponding to single frequency operation.

4.2 Frequency-Shifted Feedback (FSF-)Laser

By switching off the intracavity frequency-shift compensator of the acoustooptically tunable laser presented above its properties significantly change. During each round-trip a frequency shift is imposed on the optical field inside the resonator, which is twice the acoustical frequency of about 170 MHz. The result is a smaller but very stable output power (see Fig. 7, left) and an increased linewidth of the laser emission, which is mainly determined by the bandwidth of the acoustooptical filter (see Fig. 7, right).

As a consequence, the spectral width of the output should grow with increasing filter bandwidth. Driving the acoustooptical filter not only by one RF-signal but by two (or more) signals of neighbouring frequencies simultaneously the filter response will be broadened (more general: the Fourier spectrum of the driving RF-signals determine the filter response). This was recently investigated yielding very interesting results [19]. As an example, Fig. 8 shows

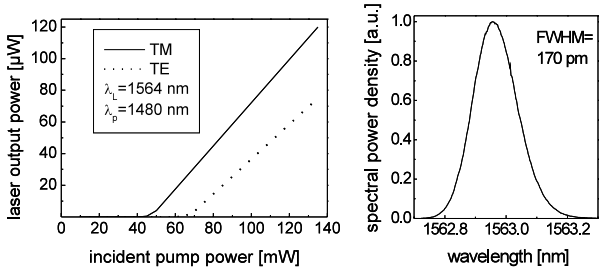

Fig. 7 Power characteristics for both polarizations (left) and emission spectrum (right) of the integrated FSF-laser.

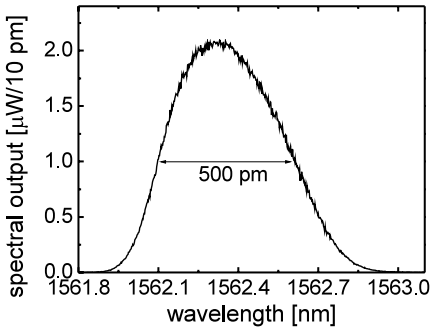

Fig. 8 Emission spectrum of the integrated FSF-laser, operated with two RF-signals of frequencies of 170.5600 MHz and 171.1755 MHz simultaneously; RF-power levels are 18.4 dBm and 17.2 dBm, respectively.

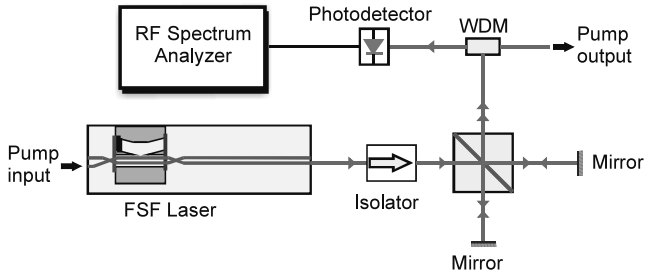

Fig. 9 Michelson interferometer operated with an integrated optical FSF-laser.

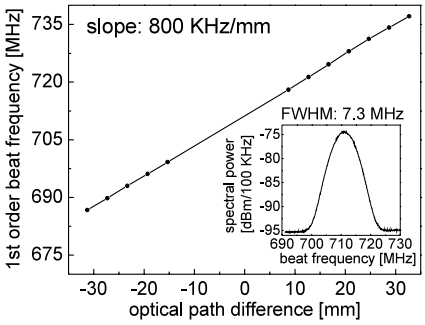

Fig. 10 Optical frequency ranging with the integrated optical FSF-laser: first order beat frequency as function of the optical path difference of both interferometer arms.

the emission spectrum if two signals of 615.5 kHz frequency difference are applied simultaneously. A broadening by a factor of three is observed, which means that the coherence length of the laser output is reduced correspondingly. In other words: the integrated FSF-laser allows to adjust the coherence properties of its output by controlling the spectral response of the acoustooptical filter.

The output spectrum of the laser as displayed in Fig. 7, if operated with one RF-signal only, should consist of a comb of narrow lines of constant frequency spacing (corresponding to the free spectral range of the laser cavity, here not resolved). The specialty of the FSF-laser is, that this comb changes with time, as previously obversed with a bulk laser [20]. If operated with two or more RF-signals of different frequencies simultaneously, the spectral fine structure and its dynamics become even more complicated. Many of the unique spectral properties of frequency shifted feedback lasers have been studied by several groups investigating bulk devices [20], [21]. However, a detailed characterization of the spectral fine structure of the integrated optical FSF-laser is still to be done [19].

With bulk FSF-lasers a variety of attractive applications has already been demonstrated such as chromatic dispersion and polarization mode dispersion measurements in fibers as well as optical frequency domain ranging [22]. Using the integrated optical FSF-laser to operate a Michelson interferometer optical frequency domain ranging has just been demonstrated as well. Figure 9 shows the experimental setup to measure the optical path difference of both interferometer arms in a very simple way. As the frequency comb of the laser emission changes with time, a superposition of the two beams propagating through the two arms of the interferometer yields various beat frequencies, which are measured by a high bandwidth photodiode. The resulting RF-spectrum is displayed by an RF-spectrum analyzer. If the first order beat frequency is used i.e. the difference frequency of two neighbouring lines corresponding to the free spectral range of the laser resonator, a resolution of < 1 mm has been achieved (see Fig. 10).

5. Ring Lasers

Recently, the first integrated optical ring laser has been demonstrated, fabricated in an Er-doped substrate [8]. Its structure is shown in Fig. 11. It consists of the Er-doped ring and two straight waveguides tangential to the ring forming two directional couplers. One serves as pump coupler allowing to couple the pump light ($\lambda = 1.48\,\mu$m) clockwise and counter-clockwise into the ring. The other one serves as laser output coupler allowing to observe the guided spontaneous fluorescence and the laser emission, if threshold is surpassed, propagating in both directions. The absorption of the pump light in the ring can be observed indirectly via the green upconversion light excited by a three step excitation of the Er-ions (see Fig. 11).

To reduce the laser threshold a new version has just been fabricated with one straight waveguide only; in this way the resonator losses have been lowered as only one directional coupler is used. Pump and laser light are separated

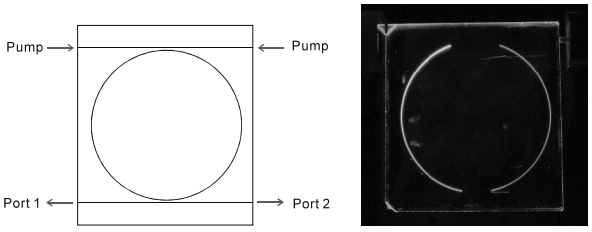

Fig. 11 Structure of the ring laser of 30 mm radius (left) and photograph of the Er-doped waveguide ring emitting green upconversion light (right).

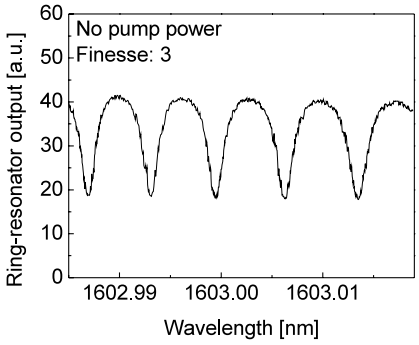

Fig. 12 Resonator response in TM-polarization without optical pumping as function of the optical wavelength.

or combined externally by appropriate fiber optical wavelength division multiplex (WDM-)devices.

First, the resonator properties were investigated with a tunable extended cavity (ECL-) semiconductor laser at λ = 1650 nm i.e. in a wavelength range without any absorption by the Er-ions; a finesse of 6.5 was observed. Taking waveguide losses of 0.15 dB/cm into account a coupling efficiency of 28% of the directional coupler could be derived (TM-polarization). Around λ = 1603 nm a reduced finesse of about 3 was measured (see Fig. 12); this reduction is due to the residual absorption by the Er-ions at this wavelength.

If pumped by a laser diode of λ_p = 1480 nm wavelength in TE-polarization (to get a better coupling efficiency for the pump and in this way a higher optical gain) the observed finesse grows as function of the pump power before lasing sets in (see Fig. 13).

Lasing starts at about 70 mW pump power (λ_p = 1480 nm) coupled into the straight channel guide from one side only in TE-polarization (see Fig. 14). As the coupling efficiency of the directional coupler is estimated to be about 25% at the pump wavelength, laser threshold corresponds to about 17.5 mW pump power coupled into the ring. The laser emission is TM-polarized, mainly due to the smaller field cross section resulting in lower losses per round-trip by the directional coupler than in TE-polarization. Nevertheless, an optimization of the directional coupler(s) has still to be done to get a high coupling efficiency at the pump wavelength for TE-polarization, but a low efficiency at the laser wavelength for TM-polarization. The small slope efficiency is a consequence of the non optimized laser design.

The ring laser emits several lines with a spectral fine

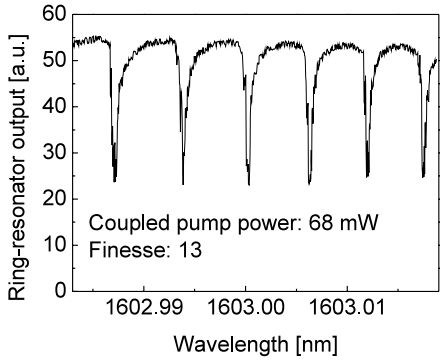

Fig. 13 Resonator response in TM-polarization with optical pumping at λ_p = 1480 nm just below laser threshold as function of the optical wavelength.

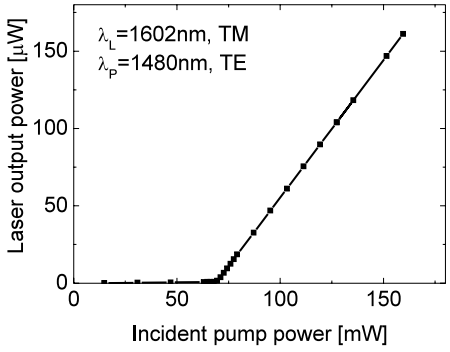

Fig. 14 Power characteristics of the integrated ring laser as output power versus pump power.

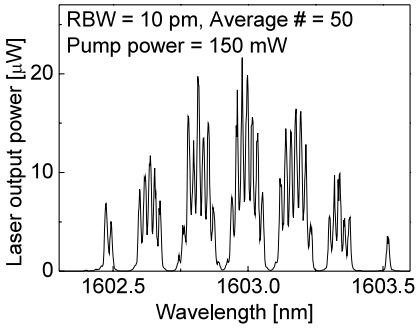

Fig. 15 Emission spectrum of the integrated optical ring laser in TM-polarization.

structure, centered around λ = 1603 nm (see Fig. 15). As the laser is operated without any wavelength selective intracavity components its emission wavelength corresponds to electronic transitions of lowest energy difference from the $^4I_{13/2}$ to the $^4I_{15/2}$ manifolds of Er^{3+} in $LiNbO_3$. For these energy levels population inversion is obtained at lowest pump power; this mode of operation is similar to that of a standard 4-level laser-system. Thus the long wavelength emission of this laser is understood; however, its spectral structure is not.

The laser emission was observed via both outputs of the straight channel investigating in this way the clockwise

and counter-clockwise propagation in the ring; both power and spectral characteristics look very similar.

6. Conclusions

The recent progress in the field of Ti:Er:$LiNbO_3$ waveguide lasers with emission wavelengths in the range 1530 nm < λ < 1603 nm has been reviewed. Narrow bandwidth DBR- and DFB-lasers increase the potential of $LiNbO_3$ integrated optics significantly; they can be incorporated everywhere in an optical circuit by spatially selective Er-doping. Acoustooptically tunable lasers promise single frequency emission and mode-hop free continuous tuning. As frequency shifted feedback devices attractive applications become possible such as optical frequency domain ranging. Ring lasers might allow the development of compact optical gyroscopes of high performance. Moreover, if fabricated in a periodically poled substrate the laser can be combined with a nonlinear device in the same waveguide enabling e.g. the development of self-frequency doubling lasers or of parametric oscillators with integrated pump.

Acknowledgment

The support of this work by the Deutsche Forschungsgemeinschaft within the programme of the research unit "Integrated optics in Lithium Niobate: New Devices, Circuits and Applications" is gratefully acknowledged.

References

[1] C. Becker, T. Oesselke, J. Pandavenes, R. Ricken, K. Rochhausen, G. Schreiber, W. Sohler, H. Suche, R. Wessel, S. Balsamo, I. Montrosset, and D. Sciancalepore, "Advanced Ti:Er:$LiNbO_3$ waveguide lasers," IEEE J. Sel. Top. Quantum Electron., vol.6, no.1, pp.101–113, 2000.

[2] I. Baumann, S. Bosso, R. Brinkmann, R. Corsini, M. Dinand, A. Greiner, K. Schäfer, J. Sochtig, W. Sohler, H. Suche, and R. Wessel, "Er-doped integrated optical devices in $LiNbO_3$," IEEE J. Sel. Top. Quantum Electron., vol.2, no.2, pp.355–366, 1996.

[3] B.K. Das, H. Suche, and W. Sohler, "Single-frequency Ti:Er:$LiNbO_3$ distributed Bragg reflector waveguide laser with thermally fixed photorefractive cavity," Appl. Phys. B, vol.73, pp.439–442, 2001.

[4] B.K. Das, R. Ricken, and W. Sohler, "Integrated optical distributed feedback laser with Ti:Fe:Er:$LiNbO_3$ waveguide," Appl. Phys. Lett., vol.82, pp.1515–1517, 2003.

[5] B.K. Das, R. Ricken, V. Quiring, H. Suche, and W. Sohler, "Distributed feedback-distributed Bragg reflector coupled cavity laser with a Ti:(Fe):Er:$LiNbO_3$ waveguide," Opt. Lett., vol.29, pp.165–167, 2004.

[6] S. Reza, H. Herrmann, V. Quiring, R. Ricken, K. Schäfer, H. Suche, and W. Sohler, "Acousto-optically tunable integrated Ti:Er:$LiNbO_3$ laser," Conference on Lasers and Electro-Optics/Europe, Munich ICM, Germany, no.CL1-5-THU, June 2003.

[7] S. Reza H. Herrmann, V. Quiring, R. Ricken, K. Schäfer, H. Suche, and W. Sohler, "Frequency shifted feedback Ti:Er:$LiNbO_3$ waveguide laser of wide tunability," Proc. 11th European Conference on Integrated Optics, pp.167–170, Prague, Czech Republic, April 2003.

[8] W. Sohler. B. Das, S. Reza, and R. Ricken, "Recent progress in integrated rare-earth doped $LiNbO_3$ waguide lasers," Technical Digest, 9th OptoElectronics and Communications Conference, no.14F4-1, p.568, Yokohama, Japan, July 2004.

[9] I. Baumann, R. Brinkmann, M. Dinand, W. Sohler, L. Beckers, C. Buchal, M. Fleuster, H. Holzbrecher, H. Paulus, K.-H. Müller, T. Gog, M. Materlik, O. Witte, H. Stolz, and W. von der Osten, "Erbium incorporation in $LiNbO_3$ by diffusion-doping," Appl. Phys. A, vol.64, pp.33–44, 1997.

[10] M. Fleuster, C. Buchal, E. Snoeks, and A. Polman, "Rapid thermal annealing of MeV erbium implanted $LiNbO_3$ single crystals for optical doping," Appl. Phys. Lett., vol.65, no.2, pp.225–227, 1994.

[11] J. Frangen, H. Herrmann, R. Ricken, H. Seibert, W. Sohler, and E. Strake, "Integrated optical, acoustically tunable wavelength filter," Electron. Lett., vol.25, no.23, pp.1583–1584, 1989.

[12] C.A. Cino, S. Riva-Sanseverino, M. De-Micheli, K. El-Hadi, F. Cusso, and G. Lifante, "Proton exchange, anneal proton exchange, and reverse proton exchange waveguides in Er:$LiNbO_3$," Proc. SPIE, vol.3280, pp.152–160, 1998.

[13] G.E. Peterson, A.M. Glass, and T.J. Negran, "Control of the susceptibility of lithium niobate to laser-induced refractive index changes," Appl. Phys. Lett., vol.19, pp.130–132, 1972.

[14] H.G. Festl, P. Hertel, E. Krätzig, and R. von Baltz, "Investigations of the photovoltaic tensor in doped $LiNbO_3$," Phys. Stat. Sol. (b), vol.113, pp.157–162, 1982.

[15] B. Das, "Integrated optical distributed Bragg refelctor and distributed feedback lasers in Er:$LiNbO_3$ waveguides with photorefractive gratings," Ph.D. Thesis, Department of Physics, University of Paderborn, Germany, 2003.

[16] C. Becker, A. Greiner, T. Oesselke, A. Pape, W. Sohler, and H. Suche, "Integrated optical Ti:Er:$LiNbO_3$ DBR-laser with fixed photorefractive grating," Topical Meeting on Integrated Photonic Research (IPR '98), Victoria/Canada, OSA Technical Digest Series, vol.4, p.304, 1998.

[17] J. Hukriede, I. Nee, D. Kip, and E. Krätzig, "Thermally fixed reflection gratings for infrared light in $LiNbO_3$:Ti:Fe channel waveguides," Opt. Lett., vol.23, pp.1405–1407, 1998.

[18] K. Schäfer, I. Baumann, W. Sohler, H. Suche, and S. Westenhöfer, "Diode-pumped and packaged acoustooptically tunable Ti:Er:$LiNbO_3$ waveguide laser of wide tuning range," IEEE J. Quantum Electron., vol.33, no.10, pp.1636–1641, 1997.

[19] S. Reza, et al., to be published

[20] K. Kasahara, K. Nakamura, M. Sato, and H. Ito, "Dynamic properties of an all solid-state frequency-shifted feedback laser," IEEE J. Quantum Electron., vol.34, no.1, pp.190–203, 1998.

[21] M. Stellpflug, G. Bonnet, B. Shore, and K. Bergmann, "Dynamics of frequency shifted feedback lasers: Simulation studies," Opt. Express, vol.11, pp.2060–2080, 2003.

[22] K. Nakamura, T. Hara, M. Yoshida, T. Miyahara, and H. Ito, "Optical frequency domain ranging by a frequency-shifted feedback laser," IEEE J. Quantum Electron., vol.36, no.3, pp.305–316, 2000.

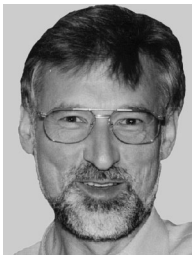

Wolfgang Sohler received the Diplom-Physiker and Dr.rer.nat. degrees in physics from the University of Munich, Germany, in 1970 and 1974, respectively. From 1975 to 1980 he was with the University of Dortmund, Germany, working on integrated optics. In 1980 he joined the Fraunhofer Institut für Physikalische Meßtechnik, Freiburg, Germany, as head of the Department of Fiber Optics. Since 1982 he has been with the University of Paderborn, Germany, as Professor of Applied Physics. His research interests include integrated optics, fiber optics and laser physics.

Bijoy K. Das received the M.Sc. degree in Physics from Vidyasagar University, India in 1995. Then he started his research in Integrated Optics with Lithium Niobate at the Indian Institute of Technology, Kharagpur. Since 1999 he worked at the University of Paderborn, Germany, developing photorefractive gratings and DFB- and DBR-waveguide lasers. He received a Ph.D. degree in 2003 from the University of Paderborn and continued to work as a post-doc at the Universites of Osaka, Japan, and Lehigh, USA.

Dibyendu Dey is currently an Integrated Master student of Physics at Indian Institute of Technology Kanpur, India. During May-July 2004, he worked within the Applied Physics group of the University of Paderborn, Germany, to study integrated Er-doped $LiNbO_3$ ring lasers.

Selim Reza received M.Sc. (Tech.) degree in Applied Physics from University of Calcutta, India in 1995 and M.S. degree in Electrical Engineering from Indian Institute of Technology, Kharagpur in 2000. Currently he is working on acoustooptically tunable lasers in Erbium doped Lithium Niobate as a Ph.D. student in the Applied Physics group of the University of Paderborn, Germany.

Hubertus Suche received the Diplom-Physiker- and Dr. rer. nat.-degrees in physics from the University of Dortmund, Germany, in 1978 and 1981, respectively. In 1981 he joined the Fraunhofer Institut für Physikalische Meßtechnik, Freiburg, Germany, as a research member in the Department of Fibre Optic Sensors. Since 1982 he is with the University of Paderborn, Germany. His research interests include nonlinear integrated optics, laser physics and material science.

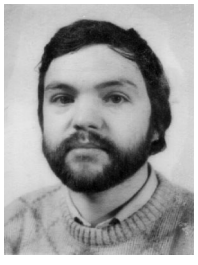

Raimund Ricken was born in Essen, Germany in 1956. He studied physics at the University of Essen and received the Diplom-Physikingenieur degree in 1983. He then joined the University of Paderborn working in the technology laboratory of the Department of Physics on the fabrication of integrated optical devices and circuits.